Extended Abstracts of the 2017 International Conference on Solid State Devices and Materials, Sendai, 2017, pp683-684

N-7-04 (Late News)

Cryogenic DC and RF Characteristics of InGaAs/InAs/InGaAs Channel HEMTs

Akira Endoh[1], Issei Watanabe[1], Akifumi Kasamatsu[1] and Takashi Mimura[1,2]

[1] National Institute of Information and Communications Technology (NICT)
4-2-1 Nukui-kitamachi, Koganei-shi, Tokyo 184-8795, Japan
Phone: +81-42-327-7256 E-mail: aendoh@nict.go.jp
[2] Fujitsu Laboratories Ltd.
10-1 Morinosato-Wakamiya, Atsugi-shi, Kanagawa 243-0197, Japan

Abstract

We fabricated $In_{0.7}Ga_{0.3}As/InAs/In_{0.7}Ga_{0.3}As$ and $In_{0.7}Ga_{0.3}As$ channel HEMTs and measured their DC and RF characteristics at 300 and 16 K. The drain-source current I_{ds} of InGaAs/InAs/InGaAs channel HEMT is more than twice that of InGaAs channel HEMT. The cutoff frequency f_T value increases by about 15 to 30% with cooling from 300 K to 16 K for both HEMTs. On the other hand, the increase in f_{max} by cooling for the InGaAs/InAs/InGaAs channel HEMT is much greater than that for the InGaAs channel HEMT.

1. Introduction

InP-based InGaAs/InAs/InGaAs channel HEMTs are the fastest field effect transistors at present [1]. The record cutoff frequency f_T of 725 GHz and maximum oscillation frequency f_{max} of 1.5 THz have been reported [1]. InP HEMTs are one of the best devices for applications to cryogenic low-noise amplifiers (LNAs) [2]. DC and RF characteristics of HEMTs are improved under cryogenic conditions due to the suppression of phonon scatterings [3]. In our previous works [4-7], we measured the DC and RF characteristics of the several InGaAs channel HEMTs under cryogenic conditions.

In this work, we fabricated decananometer-gate pseudomorphic $In_{0.7}Ga_{0.3}As/InAs/In_{0.7}Ga_{0.3}As$ and $In_{0.7}Ga_{0.3}As$ channel HEMTs and measured their DC and RF characteristics at 300 and 16 K. We compared the improvement of the DC and RF characteristics of $In_{0.7}Ga_{0.3}As/InAs/In_{0.7}Ga_{0.3}As$ channel HEMTs at 16 K with that of $In_{0.7}Ga_{0.3}As$ HEMTs.

2. Experiments

Figure 1 shows the schematic cross-sectional view of the fabricated HEMTs. The epitaxial layers were grown by metal organic chemical vapor deposition (MOCVD). We fabricated InGaAs/InAs/InGaAs and InGaAs channel HEMTs. The structure of the two types of HEMTs is the same except for the channel layer.

On-wafer DC and RF measurements were carried out at 300 and 16 K. The S-parameters were measured at frequencies up to 50 GHz in 0.25 GHz steps using an HP8510C

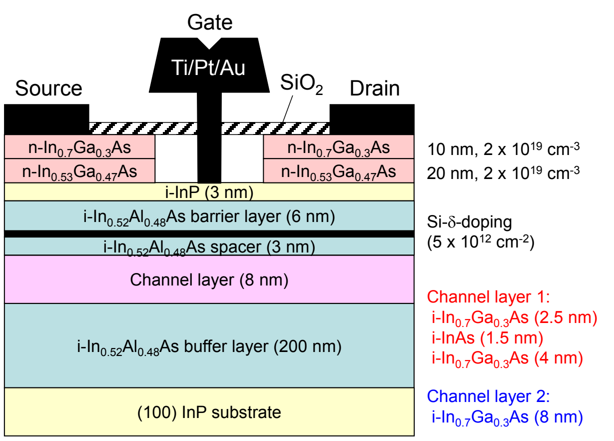

Fig. 1 Schematic cross-sectional view of InGaAs/InAs/InGaAs and InGaAs channel HEMTs.

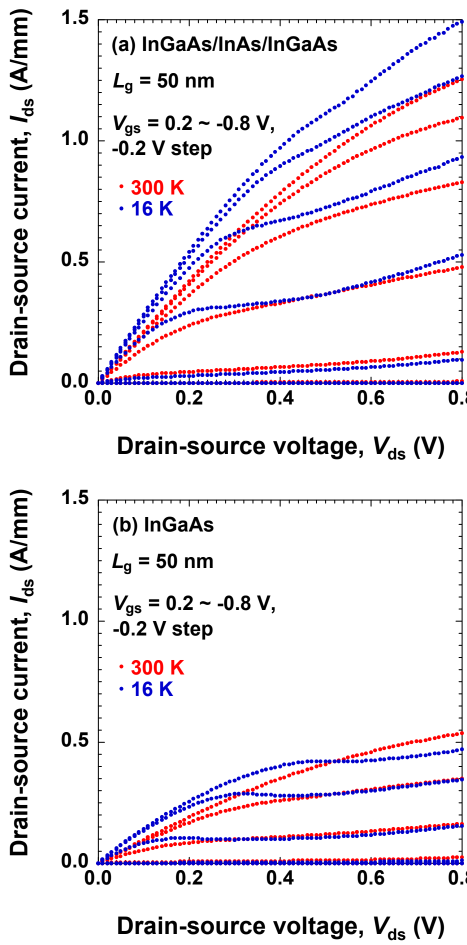

Fig. 2 Drain-source current vs. voltage (I_{ds}-V_{ds}) characteristics of 50-nm-gate InGaAs/InAs/InGaAs (a) and InGaAs (b) channel HEMTs at 300 and 16 K.

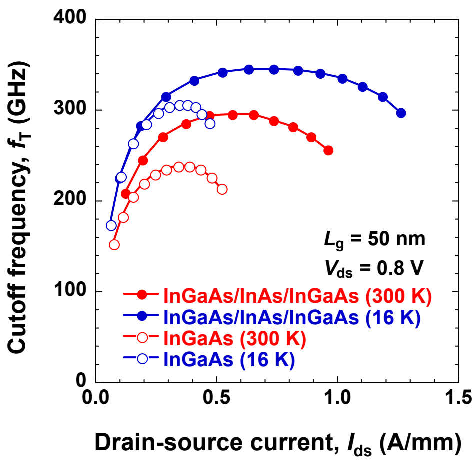

Fig. 3 Drain-source current I_{ds} dependence of cutoff frequency f_T under drain-source voltage V_{ds} of 0.8 V for 50-nm-gate InGaAs/InAs/InGaAs and InGaAs channel HEMTs at 300 and 16 K.

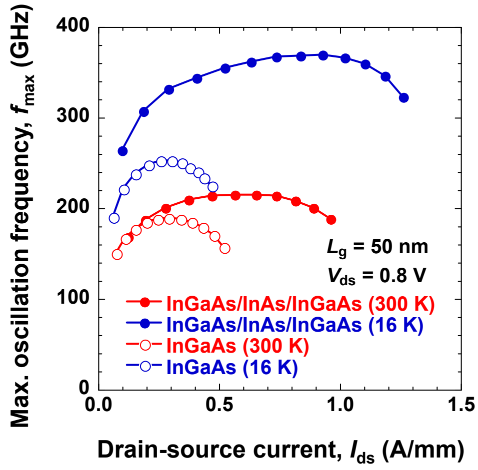

Fig. 4 Drain-source current I_{ds} dependence of maximum oscillation frequency f_{max} under drain-source voltage V_{ds} of 0.8 V for 50-nm-gate InGaAs/InAs/InGaAs and InGaAs channel HEMTs at 300 and 16 K.

vector network analyzer. Note that the parasitic capacitance due to the probing pads was subtracted from the measured S-parameters. Cutoff frequency f_T values were calculated by the extrapolation of the current gain $|h_{21}|^2$ with a slope of -20 dB/decade in the frequency range from 20 to 50 GHz. On the other hand, maximum oscillation frequency f_{max} values were obtained by the extrapolation of Mason's unilateral power gain U_g from 30 to 50 GHz.

3. Results and Discussion

Figure 2 shows the drain-source current vs. voltage (I_{ds}-V_{ds}) characteristics of 50-nm-gate InGaAs/InAs/InGaAs (a) and InGaAs (b) channel HEMTs at 300 and 16 K. These HEMTs showed good pinch-off characteristics both at 300 and 16 K. The introduction of the InAs layer resulted in a large increase in I_{ds}. The I_{ds} of InGaAs/InAs/InGaAs channel HEMT is more than twice that of InGaAs channel HEMT. In our previous work [8], the increase in I_{ds} for InGaAs/InAs/InGaAs channel HEMT was confirmed in the results of Monte Carlo simulation. Furthermore, the kink phenomenon was seen in the I_{ds}-V_{ds} characteristics for both of InGaAs/InAs/InGaAs and InGaAs channel HEMTs at 16 K [4-7].

Figure 3 shows the I_{ds} dependence of f_T for 50-nm-gate HEMTs under a V_{ds} of 0.8 V at 300 and 16 K. The f_T value increases by about 15 to 30% with cooling from 300 K to 16 K for both HEMTs. Figure 4 shows the I_{ds} dependence of f_{max} for 50-nm-gate HEMTs under a V_{ds} of 0.8 V at 300 and 16 K. The f_{max} value also increases at 16 K. For the InGaAs channel HEMT, the f_{max} value increases by about 30 to 40%. On the other hand, the increase in f_{max} is about 70 to 80% for the InGaAs/InAs/InGaAs channel HEMT. The large increase in f_{max} for the InGaAs/InAs/InGaAs channel HEMT results from the suppression of increasing drain conductance g_d. The suppression of g_d is due to the more confinement of electrons in the InAs layer by cooling.

4. Conclusions

In conclusion, we fabricated decananometer-gate pseudomorphic $In_{0.7}Ga_{0.3}As$/InAs/$In_{0.7}Ga_{0.3}As$ and $In_{0.7}Ga_{0.3}As$ channel HEMTs and measured the DC and RF characteristics at 300 and 16 K. The I_{ds} of InGaAs/InAs/InGaAs channel HEMT is more than twice that of InGaAs channel HEMT. The f_T value increases by about 15 to 30% with cooling for both HEMTs. On the other hand, the increase in f_{max} for the InGaAs/InAs/InGaAs channel HEMT is much greater than that for the InGaAs channel HEMT.

References

[1] X. B. Mei, W. Yoshida, Z. Zhou, M. Lange, J. Lee, P. H. Liu, K. Leong, R. Lai and W. R. Deal, *Extended Abstracts of the 2015 International Conference on Solid State Devices and Materials* (2015) 1034.

[2] J. Schleeh, G. Alestig, J. Halonen, A. Malmros, B. Nilsson, P. A. Nilsson, J. P. Starski, N. Wadefalk, H. Zirath and J. Grahn, IEEE Electron Device Lett. **33** (2012) 664.

[3] A. Endoh, I. Watanabe, K. Shinohara, Y. Awano, K. Hikosaka, T. Matsui, S. Hiyamizu and T. Mimura, Jpn. J. Appl. Phys. **49** (2010) 114301.

[4] A. Endoh, K. Shinohara, I. Watanabe, T. Mimura and T. Matsui, IEEE Electron Device Lett. **30** (2009) 1024.

[5] A. Endoh, I. Watanabe, T. Mimura and T. Matsui, Electron. Lett. **49** (2013) 217.

[6] A. Endoh, I. Watanabe, A. Kasamatsu, T. Takahashi, S. Shiba, Y. Nakasha, T. Iwai and T. Mimura, *Extended Abstracts of the 2015 International Conference on Solid State Devices and Materials* (2015) 220.

[7] A. Endoh, I. Watanabe, A. Kasamatsu, T. Takahashi, S. Shiba, Y. Nakasha, T. Iwai and T. Mimura, *Compound Semiconductor Week 2016* (2016) MoP-IPRM-014.

[8] A. Endoh, I. Watanabe, N. Hirose, T. Mimura and T. Matsui, *The 37th International Symposium on Compound Semiconductors* (2010) MoP28.